BBA - Bioenergetics 1865 (2024) 149492

Contents lists available at ScienceDirect

BBA - Bioenergetics

journal homepage: www.elsevier.com/locate/bbabio

Alterations in coenzyme Q_{10} status in a cybrid line harboring the 3243A>G mutation of mitochondrial DNA is associated with abnormal mitochondrial bioenergetics and dysregulated mitochondrial biogenesis

Hsiu-Chuan Yen [a,b,*], Chia-Tzu Hsu [a], Shin-Yu Wu [a], Chia-Chi Kan [a], Chun-Wei Chang [a], Hsing-Ming Chang [a], Yu-An Chien [a], Yau-Huei Wei [c], Chun-Yen Wu [a]

[a] Department of Medical Biotechnology and Laboratory Science, College of Medicine, Chang Gung University, Taoyuan, Taiwan
[b] Department of Nephrology, Chang Gung Memorial Hospital at Linkou, Taoyuan, Taiwan
[c] Center for Mitochondrial Medicine and Free Radical Research, Changhua Christian Hospital, Changhua, Taiwan

ARTICLE INFO

Keywords:
MELAS
Rotenone
Ubiquinol:ubiquinone ratio
PDSS2
COQ proteins
Mitochondrial energy deficiency

ABSTRACT

Mitochondrial DNA (mtDNA) mutations, including the m.3243A>G mutation that causes mitochondrial encephalomyopathy, lactic acidosis, and stroke-like episodes (MELAS), are associated with secondary coenzyme Q_{10} (CoQ_{10}) deficiency. We previously demonstrated that *PPARGC1A* knockdown repressed the expression of *PDSS2* and several *COQ* genes. In the present study, we compared the mitochondrial function, CoQ_{10} status, and levels of PDSS and COQ proteins and genes between mutant cybrids harboring the m.3243A>G mutation and wild-type cybrids. Decreased mitochondrial energy production, defective respiratory function, and reduced CoQ_{10} levels were observed in the mutant cybrids. The ubiquinol-10:ubiquinone-10 ratio was lower in the mutant cybrids, indicating blockage of the electron transfer upstream of CoQ, as evident from the reduced ratio upon rotenone treatment and increased ratio upon antimycin A treatment in 143B cells. The mutant cybrids exhibited down-regulation of *PDSS2* and several *COQ* genes and upregulation of *COQ8A*. In these cybrids, the levels of PDSS2, COQ3-a isoform, COQ4, and COQ9 were reduced, whereas those of COQ3-b and COQ8A were elevated. The mutant cybrids had repressed *PPARGC1A* expression, elevated ATP5A levels, and reduced levels of mtDNA-encoded proteins, nuclear DNA-encoded subunits of respiratory enzyme complexes, MNRR1, cytochrome *c*, and DHODH, but no change in TFAM, TOM20, and VDAC1 levels. Alterations in the CoQ_{10} level in MELAS may be associated with mitochondrial energy deficiency and abnormal gene regulation. The finding of a reduction in the ubiquinol-10:ubiquinone-10 ratio in the MELAS mutant cybrids differs from our previous discovery that cybrids harboring the m.8344A>G mutation exhibit a high ubiquinol-10:ubiquinone-10 ratio.

Abbreviations: AA, antimycin A; ADCK, aarF domain containing kinase; ATP5A, ATP synthase subunit α; BHA, butylated hydroxyanisole; CoQ_{10}, coenzyme Q_{10}; COX II, cytochrome *c* oxidase subunit 2; COX4I1, cytochrome *c* oxidase subunit 4 isoform 1; DAPI, 4′,6-diamidino-2-phenylindole; DHODH, dihydroorotate dehydrogenase; DMEM, Dulbecco's modified Eagle's medium; DMSO, dimethyl sulfoxide; ECAR, extracellular acidification rate; ETC, electron transport chain; FCCP, carbonyl cyanide-*p*-trifluoromethoxyphenylhydrazone; GAPDH, glyceraldehyde-3-phosphate dehydrogenase; HPLC, high-performance liquid chromatography; MELAS, mitochondrial encephalomyopathy, lactic acidosis, and stroke-like episodes; MERRF, myoclonic epilepsy with ragged-red fibers; MNRR1, mitochondrial nuclear retrograde regulator 1; mtDNA, mitochondrial DNA; MTS, mitochondrial targeting sequences; NC, nitrocellulose; ND6, NADH dehydrogenase subunit 6; nDNA, nuclear DNA; NDUFB8, NADH:ubiquinone oxidoreductase subunit B8; NDUFS2, NADH:ubiquinone oxidoreductase core subunit S2; NRF, nuclear respiratory factor; OCR, oxygen consumption rate; OXPHOS, oxidative phosphorylation; PCR, polymerase chain reaction; PDSS, decaprenyl diphosphate synthase subunit; PGC-1α, peroxisome proliferator-activated receptor-γ coactivator-1α; SDHA, succinate dehydrogenase complex flavoprotein subunit A; SDHB, succinate dehydrogenase complex iron sulfur subunit B; TFAM, mitochondrial transcription factor A; TOM20, translocase of outer mitochondrial membrane 20; UQCRC2, ubiquinol-cytochrome *c* reductase core protein 2; VDAC1, voltage-dependent anion channel 1.

* Corresponding author at: Department of Medical Biotechnology and Laboratory Science, Chang Gung University, No. 259, Wenhwa First Road, Guishan Dist., Taoyuan 33302, Taiwan.
E-mail address: yen@mail.cgu.edu.tw (H.-C. Yen).

https://doi.org/10.1016/j.bbabio.2024.149492
Received 25 April 2024; Received in revised form 19 June 2024; Accepted 27 June 2024
Available online 1 July 2024

1. Introduction

Oxidative phosphorylation (OXPHOS) involves the coupling of electron transport chain (ETC) and ATP production at Complex V (ATP synthase). ETC consists of respiratory enzyme complexes I, II, III, and IV and the two mobile electron carriers, cytochrome *c* and coenzyme Q (CoQ). CoQ accepts electrons from Complexes I and II and transfers electrons to Complex III, whereas cytochrome *c* accepts electrons from Complex III and transfers electrons to Complex IV. Subunits of these complexes are encoded by nuclear DNA (nDNA) and mitochondrial DNA (mtDNA) [1,2]. Human mtDNA is a circular DNA molecule with approximately 16,569 base pairs in the mitochondrial matrix. The 13 polypeptides encoded by mtDNA are a part of the subunits in Complexes I, III, IV, and V of OXPHOS. Cybrids have been used to demonstrate how a specific mtDNA mutation can cause abnormal biochemical phenotypes by excluding the factor of different nuclear backgrounds [3]. Mitochondrial encephalomyopathy, lactic acidosis, and stroke-like episodes (MELAS), which is primarily caused by the m.3243A>G mutation in the *MT-TL1* gene coding for $tRNA^{Leu(UUR)}$, and myoclonic epilepsy with ragged-red fibers (MERRF), which is primarily caused by the m.8344A>G mutation in the *MT-TK* gene coding for $tRNA^{Lys}$, are the two commonly encountered diseases involving impaired synthesis of mtDNA-encoded proteins [4,5]. The m.3243A>G and m.8344A>G mutations have been indicated to impair taurine modification at the wobble positions of the affected tRNAs [6,7]. Consequently, the m.3243A>G mutation was indicated to cause the defective translation of UUG-rich genes, particularly the gene for ND6 of Complex I in MELAS; whereas the m.8344A>G mutation causes defects in decoding both AAA and AAG codons and therefore whole mitochondrial translation in MERRF [6,7]. The hypothesis that the m.3243A>G mutations causes lower aminoacyl-$tRNA^{Leu(UUR)}$ and greater reduction in ND3 and ND6 levels has also been proposed [7]. However, various OXPHOS-related abnormalities have been reported in cybrids harboring the m.3243A>G mutation [8–13]. Reduced levels of translation products for all 13 mtDNA-encoded polypeptides have been shown in cybrids harboring a high percentage of the m.3243A>G mutation [11].

CoQ can exist in the oxidized form (ubiquinone of CoQ) and reduced form (ubiquinol or $CoQH_2$). Depending on the number of isoprenoid units in the polyisoprenoid tail on the benzoquinone ring, CoQ primarily exists as CoQ_6, CoQ_9, and CoQ_{10} in the budding yeast *Saccharomyces cerevisiae*, rodents, and humans, respectively, although small amount of CoQ_{10} can also be detected in rodents [14–16]. CoQ is not only required for ETC, but also serves as coenzyme of several other enzymes, including dihydroorotate dehydrogenase (DHODH) [17], an enzyme that is located on the mitochondrial intermembrane space surface of the inner membrane required for pyrimidine biosynthesis and that requires CoQ as the electron acceptor for its catalytic activity [18]. Guaras et al. showed that antimycin A (AA) treatment and the lack of Complex III, Complex IV, or cytochrome *c* could augment ubiquinol:ubiquinone ratio ($CoQH_2$/CoQ) in mouse cells, although the results of total CoQ levels were not reported [19]. Separate detection of the reduced and oxidized forms of CoQ was rarely reported in the literature for mitochondria-related investigation concerning CoQ levels. Moreover, CoQ levels in cells or tissues are often detected by measuring levels of oxidized CoQ after lengthy sample processing procedures, in which $CoQH_2$ is easily oxidized, which may cause misleading results when $CoQH_2$ was augmented.

Ten Coq polypeptides (Coq1–Coq9 and Coq11) are required for the terminal biosynthesis of CoQ_6 in *S. cerevisiae*; however, the exact identity and function of the Coq11 protein remain uncertain. Coq1, Coq2, Coq3, Coq5, Coq6, and Coq7 have known enzymatic functions. Coq2 is a mitochondrial inner membrane protein, whereas other Coq proteins are mitochondrial matrix proteins associated with the inner membrane [14]. The human ortholog proteins of yeast Coq2–Coq9 are COQ2–COQ9, whereas the human orthologs of yeast Coq1 are PDSS1 and PDSS2 (two decaprenyl diphosphate synthase subunits) [14,15]. COQ8A and COQ8B, also named as aarF domain containing kinase 3 (ADCK3) and ADCK4, respectively, are paralog proteins in humans. Coq8 in *S. cerevisiae* and human COQ8A are indicated to be atypical kinases for regulating CoQ biosynthesis [14]. Primary CoQ deficiency disease that affects multiple organ systems in humans are caused by mutations of the *PDSS1*, *PDSS2*, *COQ2–COQ9* (excluding *COQ3*) genes [14,20,21]. However, research on human PDSS and COQ proteins are limited. We previously identified specific antibodies and proteins forms for PDSS2, COQ3, COQ4, COQ5, COQ6, COQ7, COQ8A, and COQ9 in human 143B cells. We demonstrated that these proteins are localized in the mitochondria and most of them are present in protein complexes. Furthermore, presumably, most of those proteins, as visualized through Western blotting, exist in mature proteins formed through the removal of N-terminal mitochondrial targeting sequences (MTS) from full-length precursor proteins [22–24]. We also demonstrated that *COQ7* knockdown caused not only decreased CoQ_{10} level but also increased ubiquinol-10:ubiquinone-10 ratio in the 143B cells [23].

Secondary CoQ_{10} deficiency in patients with pathogenic mutations in mtDNA, including the mutations of m.3243A>G and m.8344A>G [25] and mtDNA depletion syndrome [26], have been reported. A decrease in CoQ_{10} levels has been found in cultured skin fibroblasts and cybrids with a high percentage of the m.3243A>G mutation [27]. However, in that study, the method used to measure CoQ_{10} did not differentiate between ubiquinol-10 and ubiquinone-10, and the PDSS and COQ proteins or genes were not detected. Moreover, mitochondrial bioenergetic status and OXPHOS-related proteins were not examined in the cybrids. Our previous studies revealed that decreased mitochondrial membrane potential and mitochondria-dependent ATP production in 143B cells treated with carbonyl cyanide-*p*-trifluoromethoxyphenylhydrazone (FCCP) and in MERRF cybrids harboring the m.8344A>G mutation were associated with lower total CoQ_{10} levels and decreased protein levels of PDSS2 and several COQ proteins, even when the expression of several PDSS and COQ gens was upregulated [22,23,28]. We therefore hypothesized that severe mitochondrial dysfunction suppresses the formation of mature PDSS and COQ proteins, and consequently, leads to secondary CoQ_{10} deficiency [22–24]. This deficiency develops because mitochondrial membrane potential or ATP are crucial for the import and processing of most mitochondrial matrix proteins and mitochondrial membrane potential is also required for the import of many mitochondrial inner membrane proteins [29]. Precursor proteins that are not imported tend to be degraded in the cytosol [30]. The hypothesis is also relevant to the findings that lower levels of CoQ_{10} and several COQ proteins are associated with mitochondrial abnormalities in high-grade human astrocytoma tissues [31] and in knockout mice lacking leucine-rich pentatricopeptide repeat containing protein, which is crucial for the stability of mRNA from transcription of mtDNA [32]. Furthermore, we discovered that the ubiquinol-10:ubquinone-10 ratio was not affected by FCCP treatment [23], but that the ratio was increased by the m.8344A>G mutation, which could be caused by the blockage of electron transfer that occurs after the CoQ site in ETC because of the nearly complete disappearance of mtDNA-encoded subunit II of cytochrome *c* oxidase (COX II), a subunit of Complex IV [22].

Peroxisome proliferator-activated receptor-γ coactivator-1α (PGC-1α) is regarded as a master regulator of mitochondrial biogenesis, acting as a coactivator with several transcription factors that promote the transcription of the genes encoding cytochrome *c*, subunits of OXPHOS complexes, proteins for mitochondrial protein import, and mitochondrial transcription factor A (TFAM) for regulating the copy number of mtDNA, etc. [33–36]. We previously demonstrated that the transient knockdown of the *PPARGC1A* gene, which encodes PGC-1α, resulted in the decreased expression of *PDSS2*, *COQ3*, *COQ4*, *COQ6*, *COQ8A*, and *COQ9* genes in 143B cells [37]. Decreased protein level of PGC-1α in a cybrid line with the m.3243A>G mutation has been reported [38]. Mitochondrial nuclear retrograde regulator 1 (MNRR1), also called coiled-coil-helix-coiled-coil-helix domain containing 2 (CHCHD2), is a stress regulator that can stimulate respiration by binding to COX, and it

can translocate to the nucleus to act as a transcription factor [39,40]. One study showed that MNRR1 levels were dramatically decreased in a cybrid line carrying 73 % of the m.3243A>G mutation and that MNRR1 overexpression increased the protein levels of PGC-1α, TFAM, and voltage-dependent anion channel 1 (VDAC1) in the mutant cybrids [41].

In the present study, a cybrid cell line containing the m.3243A>G mutation (Lu04 cells) and the corresponding wide-type control cybrid line (Lu02 cells), which were previously constructed in another study [42], were used to investigated the association between defective bioenergetic function and secondary CoQ_{10} deficiency in MELAS. Bioenergetic status was first characterized to confirm the mitochondrial dysfunction in Lu04 cybrids. ND6 and COX II were also detected to determine whether impaired translation of mtDNA affected the steady-state levels of mtDNA-encoded proteins in Lu04 cybrids. Second, the effects of the m.3243A>G mutation on total CoQ_{10} levels, the ubiquinol-10:ubquinone-10 ratio, mRNA levels of the *PPARGC1A* gene, mRNA levels of various *PDSS* and *COQ* genes, and protein levels of the PDSS2 protein and various COQ proteins with available antibodies were examined. The effects of Complex I and III inhibition by rotenone and AA, respectively, on CoQ_{10} status in the 143B cells were also compared. Finally, we investigated whether any of the alterations in the levels of DHODH, cytochrome *c*, several nDNA-encoded subunits of OXPHOS complexes, and proteins regulated by PGC-1α were associated with CoQ_{10}-related changes in Lu04 cybrids.

2. Materials and methods

2.1. Cells, cell culture, and treatments

Human osteosarcoma 143B cells were cultured in Dulbecco's modified Eagle's medium (DMEM) containing 4.5 g/L glucose, 110 mg/L pyruvate, and 10 % fetal bovine serum without antibiotics; the cells were maintained in a humidified CO_2 incubator with 5 % CO_2 and 95 % air at 37 °C. The Z2 Coulter Counter (Beckman Coulter) was used to count the number of trypsinized cells. To treat the 143B cells, stock solutions of rotenone and AA were prepared in dimethyl sulfoxide (DMSO) and ethanol, respectively, and filtered through a syringe filter. The stock solutions were further diluted with culture medium before use. The control groups for the rotenone treatment and AA treatment contained 0.0008 % DMSO and 0.025 % ethanol, respectively, which were equivalent to the concentrations of solvents in the treatment groups.

The wild-type Lu02 cybrids and mutant Lu04 cybrids used in the present study were previously produced by Liu et al. [42] through the fusion of 143B-ρ^0 cells with cytoplasts derived from the skin fibroblasts of a MELAS patient with heteroplasmic m.3243A>G mutation and the subsequent isolation of cybrid clones. On the basis of the results they obtained by conducting restriction fragment length polymorphism analysis after polymerase chain reaction (PCR), Liu et al. verified the absence of the m.3243A>G mutation in Lu02 cybrids and the presence of 80 % of the mtDNA with m.3243A>G mutation in Lu04 cybrids [42]. After obtaining the cybrids, we confirmed that the percentage of the mutations in the Lu04 cybrids was maintained at a nearly homoplasmic level through direct sequencing during our study (Supplemental Fig. S1). Cybrids were maintained in DMEM containing 50 mg/L uridine, which was required to grow ρ^0 cells lacking mtDNA because of possible DHODH dysfunction [43], because Lu04 cybrids grew slower in the medium without uridine and uridine did not affect the growth of Lu02 cybrids. In the medium containing 50 mg/L uridine, the Lu04 cybrids still grew more slowly than did the Lu02 cybrids. For comparative purposes, a medium containing 50 mg/L uridine was used for both cybrids in most of the experiments performed in the present study.

2.2. Evaluation of mitochondrial mass and mitochondrial membrane potential in living cells

The analysis in the present study was conducted using the ImageXpress Pico Automated Cell Imaging System (Molecular Devices, San Jose, CA, USA). Cells were grown in μ-Plate 24-well black plates with polymer coverslip bottom (ibidi GmbH, Gräfelfing, Germany). To evaluate mitochondrial mass, cells were washed with the modified Hanks balanced salt buffer solution [28], stained with the same buffer containing 500 nM nonyl acridine orange (NAO) and 4 μg/mL Hoechst 33342 dye (Thermo Fisher Scientific, Waltham, MA, USA) at 37 °C for 30 min, and were then washed again. To determine mitochondrial membrane potential, cells were stained using the same process but in the aforementioned buffer containing 2 μg/mL JC-1 (Thermo Fisher Scientific) and 4 μg/mL Hoechst 33342 dye. Hoechst 33342 was used to counter-stain the nuclei. The concentrations at which these dyes were used are identical to those applied in our previous study that used different detection methods for the same purposes [22].

For the quantification of fluorescent intensity, images from multiple scans were acquired for each well at 20× magnification by using the ImageXpress Pico Plate Imager, and average cytoplasm intensity of each well was analyzed using the CellReporterXpress software for further statistical analysis. For illustrative purposes, representative images were taken at 40× magnification for JC-1 staining. Hoechst 33342-stained nuclei were imaged by selecting the 4′,6-diamidino-2-phenylindole (DAPI) channel. The green fluorescence from NAO or JC-1 monomer was imaged using the fluorescein isothiocyanate (FITC) channel, whereas the red fluorescence from J-aggregate was imaged using the Texas Red channel. The average green fluorescent intensity of the NAO in each well was obtained to determine the mitochondrial mass. To determine mitochondrial membrane potential, the ratio of average red fluorescent intensity to average green fluoresce intensity for a well was calculated to obtain the relative mitochondrial potential of the cells in the well.

2.3. Assessment of mitochondria-dependent ATP production in whole cells

The experiments were carried out using the methods described in our previous studies [22,37]. The ATP levels of cells that were cultured in a medium containing galactose in the absence of pyruvate were measured to evaluate mitochondria-dependent ATP production; this method was employed because cells grown in galactose mostly rely on OXPHOS to produce ATP, whereas cellular ATP levels could be maintained by enhanced glycolytic activity in cells with mitochondrial defects in the presence of glucose [44]. Cells were grown in 96-well black cell culture plates. The original culture medium containing 4.5 g/L glucose and 110 mg/L pyruvate was changed to DMEM containing 1 g/L galactose without pyruvate 24 h before the cells reached confluence, after which they were analyzed for the number and ATP levels of live cells. This analysis involved the use of the MultiTox-Fluor Multiplex Cytotoxicity Assay Kit (Promega, Madison, WI, USA) to detect live-cell protease activity and the CellTiter-Glo Luminescent Cell Viability Assay Kit (Promega) to measure the ATP concentrations in instantly lysed cells. For comparison, the aforementioned experiments were also conducted for the cells incubated in a medium containing 1 g/L glucose without pyruvate for 24 h. The ATP concentrations determined through luminescence detection were normalized by the arbitrary fluorescent values that represented the cell quantity in a given well.

2.4. Analysis of OXPHOS function in cells through the Seahorse Analyzer

The OXPHOS function of cells was evaluated through the measurement of oxygen consumption rate (OCR) under the XF Cell Mito Stress Test, which was performed using the Seahorse XFp Extracellular Flux Analyzer (Seahorse Bioscience/Agilent, Santa Clara, CA, USA) in accordance with the manufacturer's protocols and the procedures described in our previous study [23]. The studied cells were plated into

XFp Miniplate microchambers and their OCR was determined under basal conditions and after the addition of oligomycin, FCCP, and rotenone plus AA sequentially. The final concentrations of the inhibitors used during the measurement were 1.0, 1.0, 0.5, and 0.5 μM for oligomycin, FCCP, antimycin A, and rotenone, respectively. The curves for OCR and extracellular acidification rate (ECAR), which indicates glycolytic flux, over time were acquired. Various parameters based on the changes in OCR across various stages, including basal respiration, ATP production-coupled respiration, maximal respiration, spare respiratory capacity (the difference between maximal respiration and basal respiration), proton leak, non-mitochondrial respiration, coupling efficiency (ATP production/basal respiration) and spare respiratory capacity as percentage (maximal respiration/basal respiration) were obtained to assess the OXPHOS function of the cells. To normalize the OCR values of each sample, the number of cells in each well was counted using the procedures described in our previous study [23]. In brief, the cells in the microchambers were trypsinized and collected. The cell pellets were then resuspended in phosphate-buffered saline, mixed with Solution 13 containing acridine orange and DAPI from ChemoMetec (Allerod, Denmark), and loaded into NC-Slide A8 chambers. To count the total number of cells, the Viability and Cell Count Assay was performed using the NucleoCounter NC-3000 (ChemoMetec) in accordance with the manufacturer's instruction.

2.5. Simultaneous analysis of steady-state levels of oxidized and reduced forms of CoQ_{10} in cells

The steady-state levels of oxidized and reduced forms of CoQ_{10} in the studied cells were analyzed using the methods described in our previous studies [22,23], with only a slight modification for the sample extraction step in the present study. Cell pellets from 2×10^6 cells were collected and stored at −80 °C. On the day of the analysis, cell pellets were homogenized in 40 μL of 50 mM sodium phosphate buffer (pH 7.4). After 10 μL of the internal standard (γ-tocopherol) in 1-propanol containing butylated hydroxyanisole (BHA) was added, 200 μL of 1-propanol with BHA was further added and mixed. The resulting supernatant after centrifugation was filtered through a syringe filter into a vial for high-performance liquid chromatography (HPLC) analysis and subsequently flushed with nitrogen gas. Several modifications were made for this part of the present study; specifically, we reduced the amount of 1-propanol used and did not perform further concentration through nitrogen flushing after centrifugation, thereby shortening the sample processing time and minimizing the chance of $CoQ_{10}H_2$ oxidation. Next, the ubiquinol-10 and ubiquinone-10 in the cells alone with γ-tocopherol (which was added into the samples) were simultaneously detected using an HPLC system with a coulometric array detector or CoulArray HPLC (ESA Biosciences, Chelmsford, MA, USA) [23,45,46]. The settings for the eight serial electrical potentials or channels were 50, 400, 500, 700, 800, −1000, −1000, and 500 mV. The ubiquinone-10 from the samples was first reduced on Channels 6 and 7 (−1000 mV) and subsequently detected on Channel 8 (500 mV) when it was reoxidized. The ubiquinol-10 in the samples was observed at an earlier retention time relative to the ubiquinone-10 in the samples, and it was detected on Channel 2 (400 mV). The amounts of ubiquinol-10 and ubiquinone-10 in each sample were normalized to the cell number. Total CoQ_{10} levels were calculated as the sum of the ubiquinol-10 and ubiquinone-10 measurements. The ubiquionol-10:ubiquinone-10 ratio was also calculated.

2.6. Analysis of mRNA levels of PPAGC1A and various PDSS and COQ genes in cells

The isolation of total RNA from the studied cells, the generation of cDNA, and the detection of produced cDNA through a real-time polymerase chain reaction (real-time PCR) system (LightCycler System 1.5; Roche, Basel, Switzerland) were conducted in accordance with our previously established procedures [28,37]. Analyses were conducted using the LightCycler TagMan Master Kit (Roche) and Universal ProbeLibrary platform (Roche). The probes and the corresponding primers for the genes that were employed are identical to those used in our previous study [37]. The LightCycler software 4.05 (Roche) was used to quantify the mRNA levels of various target genes relative to that of *ACTB* (the gene coding for β-actin). All data are presented as ratios to one of the Lu02 group for each gene.

2.7. Western blot analysis and antibodies

Western blot analysis was conducted to detect protein levels in whole-cell lysates using the methods we previously described [23,24]. The mini gel produced by the Mini-PROTEAN 3 Cell (Bio-Rad Laboratories, Hercules, CA, USA) was used to conduct Western blot analysis. Cells were homogenized in 50 mM Tris-Cl buffer (pH 7.4) containing 0.5 % Triton X-100 and protease inhibitor cocktail and centrifuged at 1000 $\times g$ for 10 min, and the resulting supernatants were used as whole cell lysates. Proteins were separated through sodium dodecyl sulfate-polyacrylamide gel electrophoresis, transferred to nitrocellulose (NC) membranes, and visualized by staining them with 0.2 % Ponceau S dissolved in 1 % acetic acid. After destaining, the NC membranes were blocked with 5 % nonfat milk powder and reacted with primary and secondary antibodies sequentially. Chemiluminescent reagents were then incubated with the NC membranes, and the chemiluminescent signals of the protein bands on the NC membranes were recorded using the Amersham Imager 600 system (GE, Chicago, IL, USA). The intensity of protein signals was quantified using the Multi Gauge software (Fujifilm, Tokyo, Japan). The abundance of target proteins was normalized using α-tubulin as a reference for most of the experiments unless otherwise indicated. The obtained data were further converted to the ratio relative to the mean of the control group in the same set of Western blot experiment. The PageRuler Prestained Protein Ladder (#26616; Thermo Fisher Scientific) and the Precision Plus Protein Dual Color Standards (#161-0374; Bio-Rad Laboratories) were used as the protein markers.

The mouse monoclonal antibody against α-tubulin (ab7291) was purchased from Abcam (Cambridge, UK). Mouse monoclonal antibodies against cytochrome *c* oxidase subunit 4 isoform 1 (COX4I1; 66110-1-Ig) and MNRR1/CHCHD2 (66302-1-Ig) were purchased from Proteintech (Rosemont, IL, USA). Mouse monoclonal antibodies against PDSS2 (sc-515137), COQ3 (sc-376774), COQ6 (sc-393932), COQ7 (sc-376484), COQ9 (sc-365073), and DHODH (sc-166348) were purchased from Santa Cruz Biotechnology (Dallas, TX, USA). Rabbit polyclonal antibodies against COQ4 (16654-1-AP) and TFAM (22586-1-AP) were purchased from Proteintech. Rabbit polyclonal antibodies against COQ8A/CABC1 (GTX110374) and VDAC1 (GTX114187) were obtained from Gentex (Hsinchu, Taiwan). The mouse monoclonal antibody (MAB374) against glyceraldehyde-3-phosphate dehydrogenase (GAPDH) was purchased from Chemicon/Merck (Darmstadt, Germany). The rabbit monoclonal antibody against succinate dehydrogenase complex flavoprotein subunit A (SDHA) was purchased from Abcam (ab137040). The rabbit polyclonal antibody against COQ5 previously produced in our laboratory was used in the present study (24). The Total OXPHOS Human WB Antibody Cocktail (ab110411), which contains a mixture of antibodies recognizing one labile subunit of each of the five OXPHOS complexes, was purchased from Abcam. Rabbit polyclonal antibodies against mtDNA-encoded NADH dehydrogenase subunit 6 (ND6; A17991) and against NADH:ubiquinone oxidoreductase core subunit S2 (NDUFS2; A12858) and the rabbit monoclonal antibody against translocase of outer mitochondrial membrane 20 (TOM20; A19403) were purchased from ABclonal (Woburn, MA, USA). Horseradish peroxidase (HRP)-conjugated goat-anti-mouse (5220-0341) and goat-anti-rabbit (AP132P) secondary antibodies were purchased from SeraCare (Milford, MA, USA) and Chemicon/Merck, respectively.

2.8. Statistical analysis

Statistical analysis was performed using IBM SPSS statistics software version 22.0 (IBM, Armonk, NY, USA). The statistical significance of the differences between the two compared groups were evaluated by performing the two-tailed *t*-tests. One-way analysis of variance with the Tukey's honest significance test was used for the comparison among multiple groups. There were multiple independent replicates in each group. These replicates were independent samples collected from cells grown on different dishes or flasks. Differences were regarded as significant when $P < 0.05$.

3. Results

3.1. Reduction of mitochondrial membrane potential and mitochondria-dependent ATP production with unaltered mitochondrial mass in Lu04 cybrids

To characterize possible changes in the mitochondrial function in the Lu04 cybrids, we first evaluated mitochondrial mass, mitochondria-dependent ATP production, and mitochondrial membrane potential in Lu02 and Lu04 cybrids. These comparisons were conducted in both the absence and presence of uridine. The results (Fig. 1A) indicated that the mitochondrial masses of the Lu02 and Lu04 cybrids did not differ significantly. Additionally, uridine did not affect these results, as indicated by the quantification results of NAO staining. The level of ATP production after the cybrids were kept in the medium containing 1 g/L of glucose or galactose for 24 h was further evaluated (Fig. 1B). The results of this evaluation indicated that relative to Lu02 cybrids, the ability of Lu04 cybrids to produce ATP through mitochondrial OXPHOS in the presence of galactose was severely hampered. In the absence of uridine, this defect of Lu04 cybrids was worsened, whereas the ATP production of Lu02 cybrids was further stimulated. Similar changes occurred when ATP production was measured in a medium containing glucose, suggesting the lack of enhanced glycolytic responses in Lu04 cybrids. Mitochondrial membrane potential was determined by staining the cybrids with JC-1. The quantification results revealed that Lu04 cybrids exhibited considerably lower mitochondrial membrane potential relative to Lu02 cybrids, regardless of whether the cells were grown in the medium containing uridine (Fig. 1C). The representative merged images for JC-1 staining are illustrated in Fig. 1D. These results indicated that the defects in mitochondrial energy production in Lu04 cybrids were not caused by changes in mitochondrial mass. Because the alterations in Lu02 and Lu04 cybrids in both the absence and presence of uridine were similar and Lu04 grew poorly in the absence of uridine, subsequent experiments were conducted in the uridine-containing

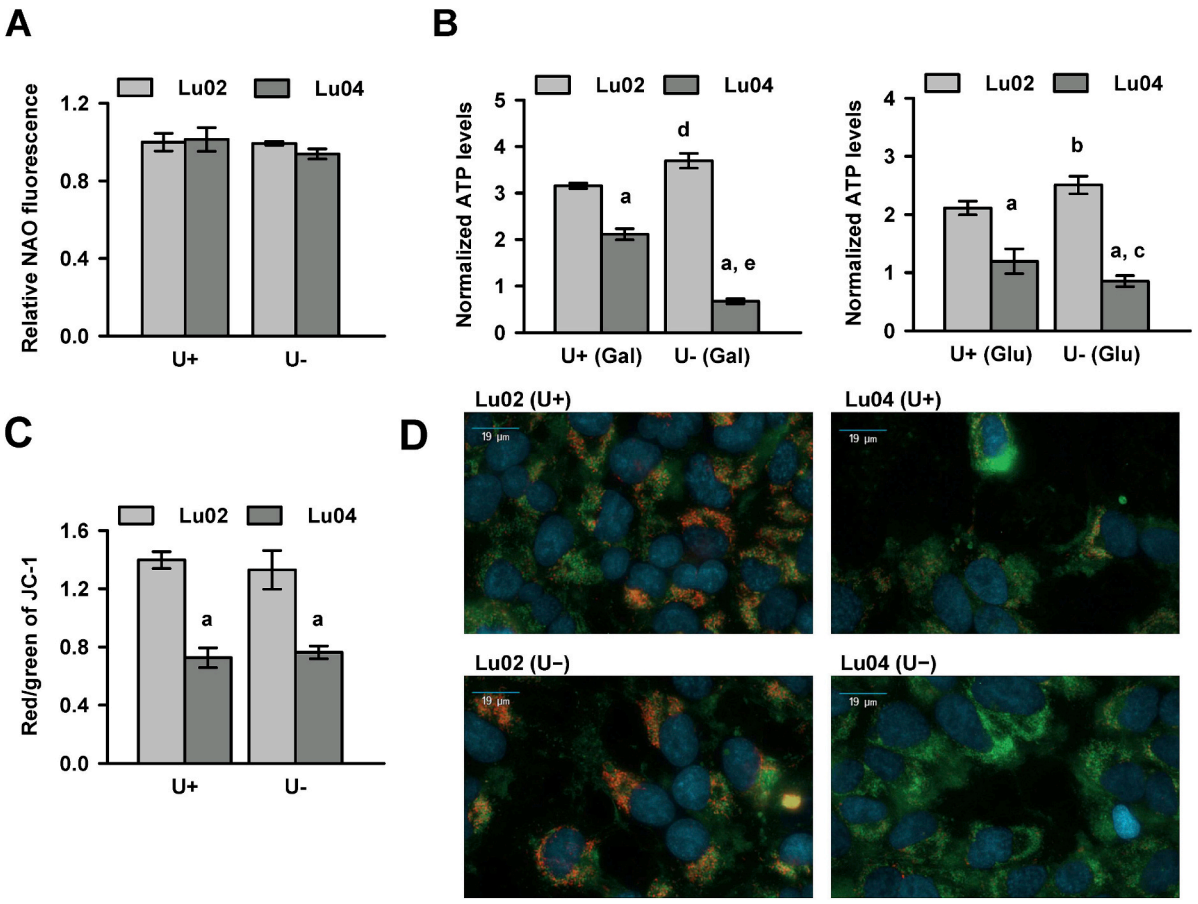

Fig. 1. Evaluation of mitochondrial mass, mitochondria-dependent ATP production, and mitochondrial membrane potential in Lu02 and Lu04 cybrids.
(A) Mitochondrial mass, which was assessed through NAO fluorescence by using the ImageExpress Pico Automated Cell Imaging System, did not differ significantly between Lu02 and Lu04 cybrids either in the presence (U+) or absence (U−) of 50 mg/L uridine. Three wells were used per group. (B) Whole-cell ATP levels in the two cybrids under the U+ and U− conditions were compared. Four wells were used per group. The comparison was made after incubating the cells for 24 h in medium containing either 1 g/L galactose (Gla) or 1 g/L glucose (Glu). $^{a}P < 0.001$ versus Lu02 cybrids under the U+ or U− condition. $^{b}P < 0.05$ versus Lu02 under the U+ condition, $^{c}P < 0.05$ versus Lu04 cybrids under the U+ condition, $^{d}P < 0.001$ versus Lu02 under the U+ condition, $^{e}P < 0.001$ versus Lu04 cybrids under the U+ condition. (C) Mitochondrial membrane potential quantified on the basis of the red/green fluorescence ratio of JC-1. Four wells were used per group. $^{a}P < 0.001$ versus Lu02 cybrids under the U+ or U− condition. No difference was noted between the U+ and U− conditions for either cybrid. (D) Representative merged images for JC-1 staining, which were acquired using the ImageExpress Pico Automated Cell Imaging System.

medium for both types of cybrids.

3.2. Defective OCR profiles in Lu04 cybrids as determined by Mito Stress Test

Furthermore, we conducted the Mito Stress Test with the Seahorse analyzer to determine whether the function of OXPHOS in Lu04 cybrids was defective. The curve of OCR changes over time revealed that the OCR of Lu04 cybrids was markedly lower than that of Lu02 cybrids at both the basal stage and the stage after FCCP addition (Fig. 2A). The basal ECAR was similar between the two cybrids, indicating that the marked differences in OCR was not due to errors in cell counting. However, the results of ECAR curve indicated that the increase in ECAR, an indication of enhanced glycolytic activity, in response to the addition of mitochondrial inhibitors was less obvious in Lu04 cybrids than in Lu02 cybrids (Fig. 2B). The results of the XF Mito Stress Test (Fig. 2C) revealed that basal respiration, maximal respiration, ATP production-coupled respiration, spare respiratory capacity, and proton leak were significantly lower in Lu04 cybrids than those in Lu02 cybrids; but no differences in non-mitochondrial respiration was found. Additionally, the coupling efficiency and spare respiratory capacity as percentage of Lu02 and Lu04 cybrids did not differ significantly. These results indicate that in contrast to Lu02 cybrids, Lu04 cybrids exhibited multiple abnormalities in OXPHOS function, particularly defects in respiratory enzyme complexes.

3.3. CoQ_{10} levels in Lu02 and Lu04 cybrids and in 143B cells treated with rotenone and AA

To determine whether CoQ_{10} levels were lower in Lu04 cybrids than in Lu02 cybrids, we performed CoulArray HPLC analysis to simultaneously analyze the ubiquinol-10 and ubiquinone-10 contents in the cybrids. The results of Lu04 cybrids cultured in the presence of uridine was compared with Lu02 cybrids both in the presence and absence of uridine (Fig. 3). We found that both the levels of ubiquinol-10 levels and ubiquinone-10 were all lower in the Lu04 cybrids than in Lu02 cybrids; however, the decrease in the ubiquinol-10 appeared to be greater. Consequently, the total CoQ_{10} levels and ubiquinol-10:ubiquinone-10 ratio of Lu04 cybrids were both decreased. Furthermore, we confirmed that uridine did not affect the results of Lu02 cybrids.

To elucidate whether the increase of ubiquinol-10:ubiquinone-10 ratio was attributed to defects in Complex I more than in other respiratory enzyme complexes in Lu04 cybrids, we compared the effects of rotenone (a Complex I inhibitor) and AA (a Complex III inhibitor) on the ubiquinol-10:ubiquinone-10 ratio in 143B cells. The results indicated that 24 h of exposure to 0.2-μM rotenone, which did not affect cell growth or total CoQ_{10} levels, significantly reduced the ubiquinol-10:ubiquinone-10 ratio. The decrease in this ratio can be attributed to a marked increase in ubiquinone-10 levels and a slight decrease in ubiquinol-10 levels (Fig. 4A). Furthermore, treatment of the 143B cells with 10 μM AA for 6 h considerably augmented the ubiquinol-10:ubiquinone-10 ratio, which was caused by increased ubiquinol-10 levels and decreased ubiquinone-10 levels. This treatment did not cause obvious cytotoxicity, although the total CoQ_{10} levels slightly increased (Fig. 4B). Therefore, we speculate that the m.3243A>G mutation might cause the blockage of electron flux through Complex I or upstream of the CoQ site (instead of downstream of the CoQ site) on the ETC in Lu04 cybrids.

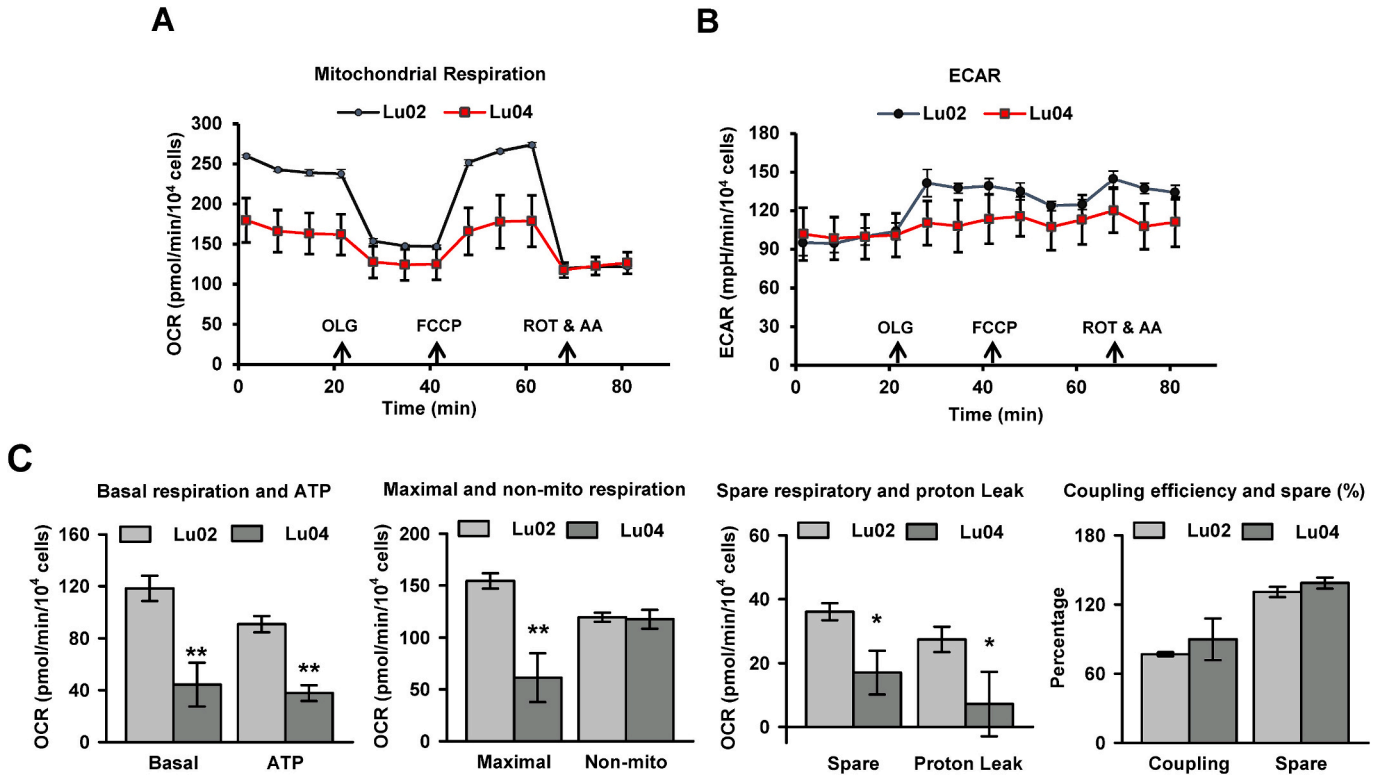

Fig. 2. Assessment of OXPHOS function in Lu02 and Lu04 cybrids by using the Seahorse XF Cell Mito Stress Test.
The two types of cybrids were cultured in the medium containing 50 mg/L uridine. There were three replicates in each group. (A) Changes in OCR over time. The arrows from the left to the right indicate the time points for the sequential addition of oligomycin (OLG), FCCP, and rotenone plus antimycin A (ROT & AA). (B) Changes in ECAR over time. (C) Key respiratory parameters, including basal respiration, maximal respiration, ATP production-coupled respiration, spare respiratory capacity, non-mitochondrial respiration, proton leak, coupling efficiency, and spare respiratory capacity, as a percentage were analyzed. *$P < 0.05$ and **$P < 0.01$ versus Lu02 cybrids.

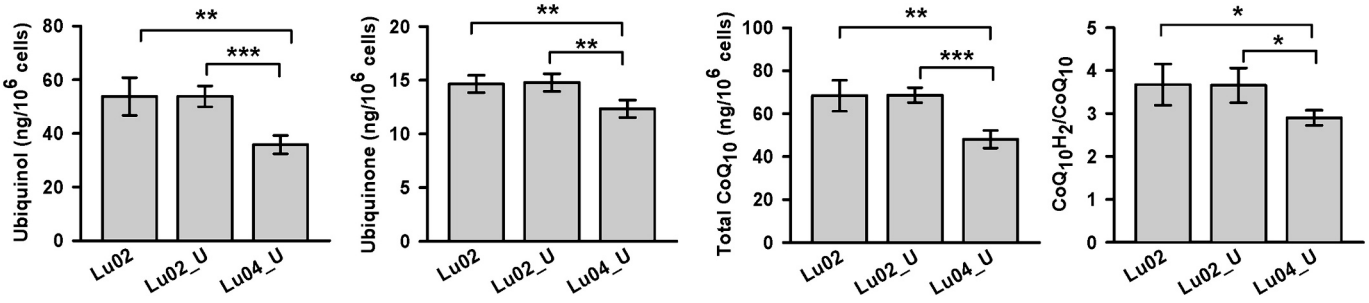

Fig. 3. CoQ_{10} status in Lu02 and Lu04 cybrids.
Comparison of ubiquinol-10 level, ubiquinone-10 level, total CoQ_{10} level, and the ubiquinol-10:ubiquinone-10 ratio ($CoQ_{10}H_2/CoQ_{10}$) between Lu04 cybrids (in the presence of 50 mg/L uridine) and Lu02 cybrids under both conditions (in the absence and presence of uridine). $^*P < 0.05$, $^{**}P < 0.01$, and $^{***}P < 0.001$ between the two indicated groups.

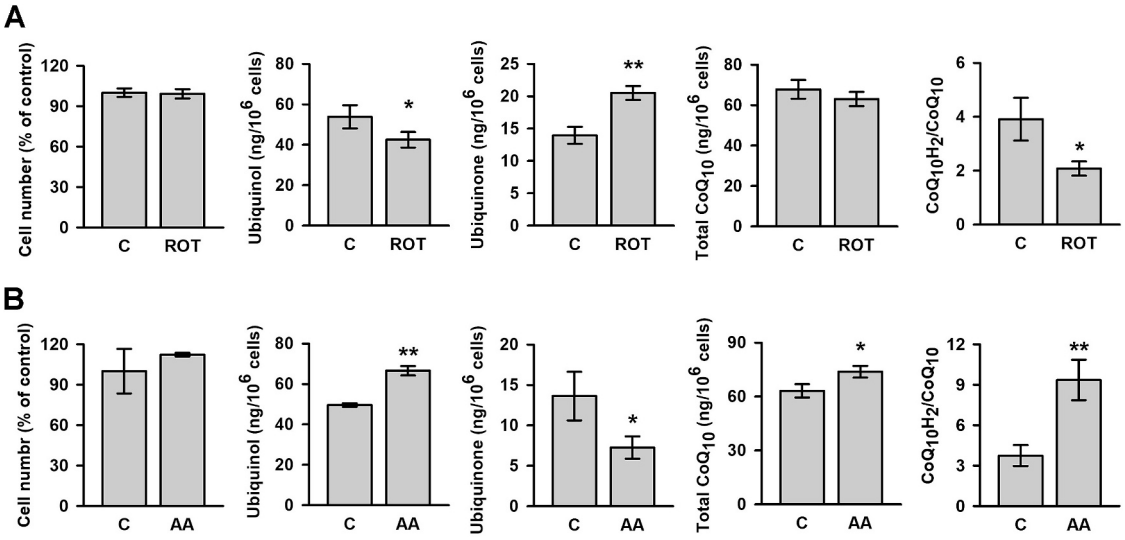

Fig. 4. Effects of rotenone and AA treatment on CoQ_{10} status in 143B cells.
The data of cell number relative control, ubiquinol-10 levels (ubiquinol), ubiquinone-10 levels (ubiquinone), total CoQ_{10} levels, and the ubiquinol-10:ubiquinone-10 ratio ($CoQ_{10}H_2/CoQ_{10}$) are presented. There were three replicates in each group. $^*P < 0.05$ and $^{**}P < 0.01$ versus control. (A) Results for rotenone treatment. Cells were treated with 0.2 μM rotenone for 24 h. (B) Results for AA treatment. Cells were treated with 10 μM AA for 6 h.

3.4. mRNA levels of various PDSS and COQ genes and PPARGC1A gene in Lu02 and Lu04 cybrids

To elucidate whether the decrease in CoQ_{10} levels in Lu04 cybrids was associated with changes in the expression of various *PDSS* and *COQ* genes, the mRNA levels of these genes in Lu02 and Lu04 cybrids were compared by conducting real-time PCR. The results (Fig. 5) indicated that the mRNA levels of *PDSS1*, *PDSS2*, *COQ3*, *COQ4*, *COQ5*, *COQ6*, *COQ7*, and *COQ9* were significantly downregulated, whereas that of *COQ2* was not significantly altered. Notably, *COQ8A* expression was markedly upregulated. Furthermore, because we have previously demonstrated that transient *PPARGC1A* knockdown could repress the expression *PDSS2* and several *COQ* genes in 143B cells [37], we measured the expression of the *PPARGC1A* gene and discovered that it was considerably lower in Lu04 cybrids than in the Lu02 cybrids.

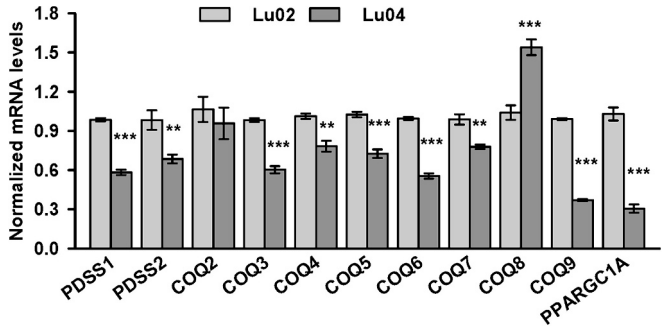

Fig. 5. mRNA levels of *PPARGC1A* and various PDSS and COQ genes in Lu02 and Lu04 cybrids.
The two types of cybrids were cultured in the medium containing 50 mg/L uridine. There were four replicates in each group. $^{**}P < 0.01$ and $^{***}P < 0.001$ versus Lu02 cybrids.

3.5. Protein levels of PDSS2 and various COQ proteins in Lu02 and Lu04 cybrids

To compare the intracellular levels of PDSS2 and various COQ proteins with available antibodies in Lu02 and Lu04 cybrids, Western blot analysis was conducted to detect the levels of those proteins in whole cell homogenates. The Western blot images and the quantification results are presented in Fig. 6A and Fig. 6B, respectively. The positions of each target protein bands relative to the protein sizing markers have been previously illustrated [22,23]. As indicated previously, the signal of PDSS2-a was too weak to be reliably quantified [23]. PDSS2-b and PDSS2-c levels were both markedly suppressed in Lu04 cybrids. COQ4 and COQ9 levels were also significantly lower in Lu04 cybrids than in

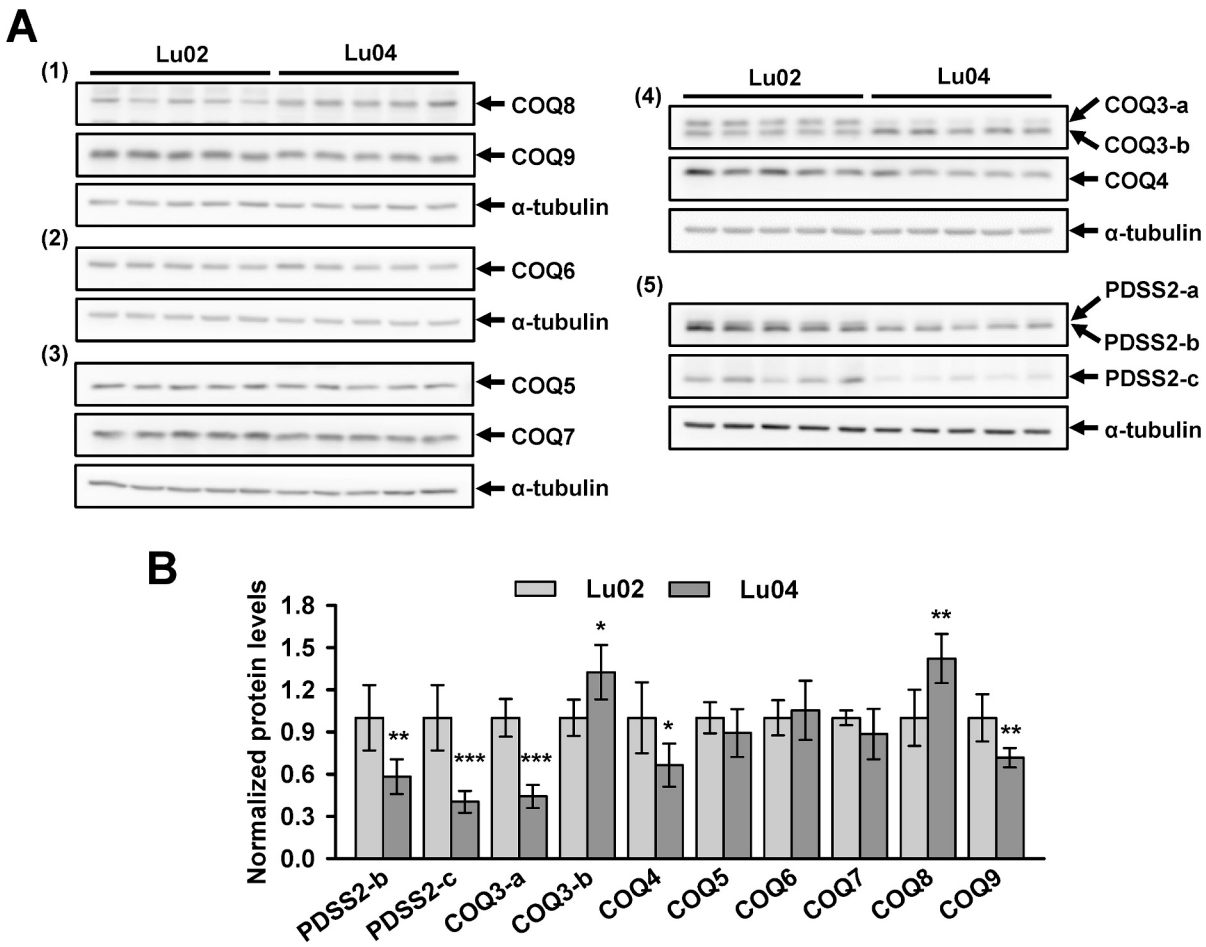

Fig. 6. Levels of PDSS2 and various COQ proteins in Lu02 and Lu04 cybrids.
The two types of cybrids were cultured in the medium containing 50 mg/L uridine. The numbers on images indicate independent blots. There were five replicates in each group. The positions of each target protein bands relative to the protein sizing markers have been previously verified and illustrated in our publications [22,23]. (A) Western blot images. (B) Quantitative analysis presented in a bar graph format. $^{*}P < 0.05$, $^{**}P < 0.01$, and $^{***}P < 0.001$ versus Lu02 cybrids.

Lu02 cybrids; however, the levels of COQ5, COQ6, and COQ7 proteins did not differ between these two types of cybrids. The levels of COQ8A were higher in Lu04 cybrids than in Lu02 cybrids. Perplexingly, in Lu04 cybrids, the COQ3-a isoform was augmented, whereas the COQ3-b isoform was suppressed.

3.6. *Levels of representative OXPHOS complex proteins, MNRR1, TFAM, VDAC1, cytochrome c, DHODH, and GAPDH in Lu02 and Lu04 cybrids*

Western blot analysis was performed to determine whether the levels of mtDNA-encoded proteins were reduced and whether changes in CoQ_{10} in Lu04 cybrids were associated with alterations in other OXPHOS-related and mitochondrial biogenesis-related proteins. Several OXPHOS subunits encoded by mtDNA and nDNA were therefore detected. PGC-1α levels in whole cell lysates were not detected because the gene coactivation function of PGC-1α is also determined by its nuclear translocation and posttranslational regulation [34,36]. Instead, protein levels of VDAC1, TFAM, cytochrome *c*, and TOM20 were examined because the genes encoding these proteins can be regulated by some of the transcriptional partners of PGC-1α [34,35,47]. MNRR1 was analyzed because it is potentially involved the regulation of PGC-1α, TFAM, and VDAC1 levels [41]. Furthermore, GAPDH, a key enzyme for glycolysis, was analyzed because of potential dysregulation of glycolysis in Lu04 cybrids, as indicated by the results presented in Figs. 1B and 2B. In addition, DHODH was analyzed because it is a mitochondrial inner membrane protein that requires mitochondrial membrane potential for its import into mitochondria and CoQ is the electron acceptor for the catalytic activity of this enzyme [18].

The Total OXPHOS Human WB Antibody Cocktail was used to simultaneously detect five subunits of OXPHOS complexes that are presumably to be labile when these complexes are not properly assembled. These subunits are listed as follows: NADH:ubiquinone oxidoreductase subunit B8 (NDUFB8), succinate dehydrogenase complex iron sulfur subunit B (SDHB), ubiquinol-cytochrome *c* reductase core protein 2 (UQCRC2), COX II, and ATP synthase subunit α (ATP5A), which correspond to Complexes I, II, III, IV, and V, respectively. Supplemental Fig. S2 depicts all five proteins on the same blot at a certain exposure time point, which also illustrates that ATP5A and SDHB exhibit the highest and second-highest abundance levels, respectively. The Western blot images and quantification results derived for the individual proteins at optimal exposure time points for reliable quantification are presented in Fig. 7A and Fig. 7B, respectively. The analysis revealed a significant reduction (70 %) in the level of mtDNA-encoded COX II in Lu04 cybrid. Regarding nDNA-encoded OXPHOS subunits, we discovered that the levels of NDUFB8, SDHB, and UQCRC2 were considerably lower in Lu04 cybrids than in Lu02 cybrids. In particular, the level of NDUFB8 in Lu04 cybrids was reduced by 83 %. However, the ATP5A level was significantly upregulated in Lu04 cybrids. For this experiment, COQ6 protein was used as the normalization reference for quantification because its level was not altered in Lu04 cybrids (Fig. 6) and the detection of tubulin was hindered by the detection of ATP5A.

The images and quantification results for the Western blot analysis of

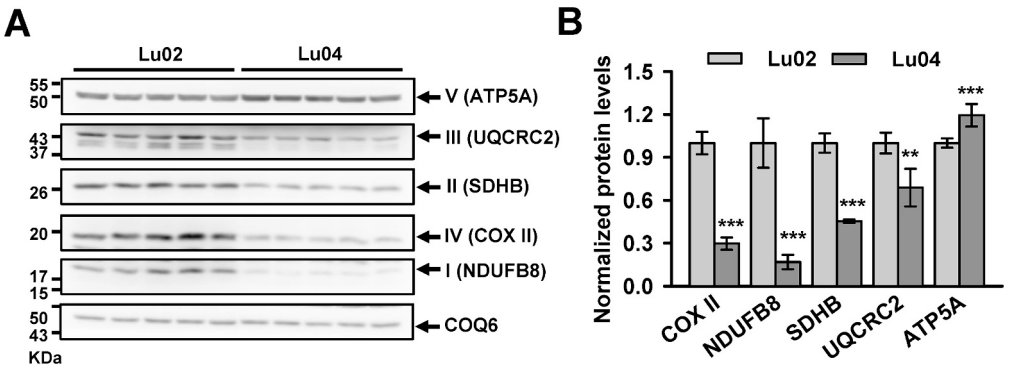

Fig. 7. Detection of representative subunits of OXPHOS complexes in Lu02 and Lu04 cybrids using the Total OXPHOS Human WB Antibody Cocktail.
The two types of cybrids were cultured in the medium containing 50 mg/L uridine. There were five replicates in each group. The subunits of the five OXPHOS complexes were simultaneously detected on the same blot (Fig. S2), but only images derived for the individual proteins at optimal exposure time points are presented and used for quantification. (A) Western blot images. (B) Quantification results depicted using a bar graph $^{**}P < 0.01$ and $^{***}P < 0.001$ versus Lu02 cybrids.

ND6 (a mtDNA-encoded subunit of Complex I), NDUFS2 (a nDNA-encoded subunit of Complex I), COX4I1 (a nDNA-encoded subunit of Complex IV), and SDHA (a nDNA-encoded subunit of Complex II), cytochrome *c*, MNRR1, TFAM, VDAC1, TOM20, DHODH, and GAPDH are presented in Fig. 8A and Fig. 8B, respectively. These results indicated that the levels of ND6, cytochrome *c* and COX4I1 were markedly reduced (by approximately 60 %) in Lu04 cybrids. The levels of NDUFS2, SDHA and DHODH levels were also significantly decreased in these cybrids. Furthermore, slight yet significant reductions were noted in the levels of MNRR1 and GAPDH levels in Lu04 cybrids. Notably, Lu02 and Lu04 cybrids did not differ significantly in terms of the level of TFAM, TOM20, or VDAC1.

4. Discussion

To the best of our knowledge, this is the first to investigate the effect of the MELAS syndrome-associated m.3243A>G mutation on the levels of ubiquinol-10, ubiquinone-10, and its biosynthetic genes and proteins using a cybrid model. We found that the mutation reduced the total CoQ_{10} levels and that the change was not attributable to any variation in mitochondrial mass. The mutation also reduced the ubiquinol-10: ubiquinone-10 ratio in Lu04 cybrids. The observed changes in CoQ_{10} status following the treatment of 143B cells with rotenone and AA indicate that the reduced ubiquinol-10:ubiquinone-10 ratio in Lu04 cybrids may be due to an increased blockage in electron transfer to the oxidized form of CoQ_{10}, likely within Complex I, relative to the electron

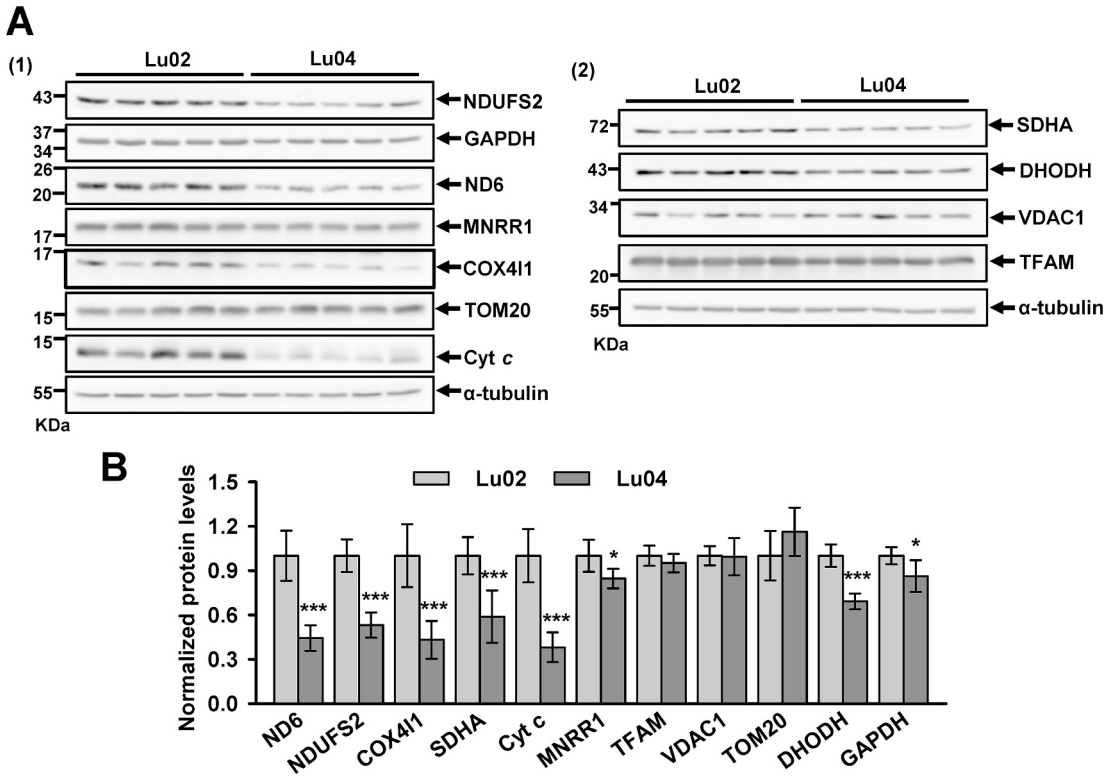

Fig. 8. Levels of ND6, NDUFS2, COX4I1, SDHA, mitochondrial biogenesis-related proteins, DHODH, and GAPDH in Lu02 and Lu04 cybrids.
The two types of cybrids were cultured in the medium containing 50 mg/L uridine. Cyt c represents cytochrome *c*. The numbers on images indicate independent blots. There were five replicates in each group. (A) Western blot images. (B) Quantification results are presented using a bar graph. $^{*}P < 0.05$ and $^{***}P < 0.001$ versus Lu02 cybrids.

flow from the reduced form of CoQ_{10} to subsequent electron carriers despite reduced levels of representative subunits across all four respiratory enzyme complexes and cytochrome *c*. Furthermore, the downregulation of *PPARGC1A* in Lu04 cybrids was associated with that of several *PDSS* and *COQ* genes. However, *COQ8* expression was upregulated. Notably, the changes in PDSS and COQ proteins were inconsistent with those in their corresponding genes. Reductions in the levels of CoQ_{10}, PDSS2, COQ3-a, COQ4, COQ9, DHODH, and subunits of several nDNA-encoded respiratory complexes in Lu04 cybrids may be partly attributable to mitochondrial energy deficiency or OXPHOS dysfunction, as indicated by the reduced mitochondrial membrane potential, suppressed mitochondria-dependent ATP production, and abnormal OCR profiles discovered in the Mito Stress Test. These changes are presumably secondary effects caused by a relatively low level of mtDNA-encoded proteins, as confirmed by a marked reduction in ND6 and COX II levels in Lu04 cybrids. Dysregulation of mitochondrial biogenesis signaling may have contributed to the secondary CoQ_{10} deficiency and defective bioenergetic function observed in Lu04 cybrids. However, the dysregulation involving PGC-1α might not have been the primary cause, given that the mitochondrial mass and levels of TFAM, TOM20, and VDAC1 levels remained unchanged while the ATP5A levels were elevated.

Decreased protein levels of mtDNA-encoded COX I or COX II, but not ND6, have often been reported in the cybrids harboring the m.3243A>G mutation [8,11] because antibodies against ND6 or other mtDNA-encoded proteins were not commercially available previously. In this study, we discovered that steady-state levels of both ND6 and COX II were reduced by 56 % and 70 %, respectively, in Lu04 cybrids. Furthermore, comprehensive assays conducted in the present study verified that Lu04 cybrids exhibited OXPHOS dysfunction and mitochondrial energy deficiency. The results of the Mito Stress Test revealed that Lu04 cybrids exhibited more extensive defects in the respiratory enzyme complexes than in Complex V or OXPHOS coupling, as evidenced by the considerably reduced OCR both before and after FCCP addition without any change in coupling efficiency. This was likely associated with reduced levels of multiple subunits of the respiratory enzyme complexes that were investigated. Lu04 cybrids maintained 30 % OCR compared with Lu02 cybrids. Reduced mitochondrial membrane potential and mitochondria-dependent ATP production were also observed in Lu04 cybrids. However, as shown in our previous study, respiration and typical OCR changes were absent and mitochondria-dependent ATP production was nearly diminished in the mutant cybrids harboring the m.8344A>G mutation, which was associated with a substantial reduction of mtDNA-encoded COX II to a negligible level [22]. Moreover, we have previously demonstrated that whole-cell ATP levels in 143B cells remained unchanged or increased in response to acute treatment oligomycin [37] or FCCP [22] treatment, respectively, when cells were cultured in a medium containing 1 g/L glucose. Conversely, ATP production in the presence of galactose was almost completely diminished after oligomycin or FCCP treatment [22,37], suggesting that the whole-cell ATP levels is not suitable to reflect the mitochondrial energy status because their reliance on enhanced glycolytic activity under mitochondrial dysfunction. However, similar reductions were noted in ATP production between Lu04 cybrids grown in the presence of galactose and those grown in the presence of glucose, suggesting a lack of compensatory ATP production through enhanced glycolysis. This hypothesis is supported by the little increase in ECAR after the addition of mitochondrial inhibitors during the Mito Stress Test and reduced GAPDH levels in Lu04 cybrids.

By simultaneously measuring the reduced and oxidized forms of CoQ_{10}, we, for the first time, revealed that both the m.3243A>G mutation and rotenone treatment led to a reduction in the ubiquinol-10:ubiquinone-10 ratio. The observed increase in this ratio after AA treatment is consistent with the findings of Guaras et al. [19]. We also previously demonstrated that FCCP treatment in 143B cells did not alter the ubiquinol-10:ubiquinone-10 ratio, whereas the m.8344A>G mutation caused an increase in this ratio [23]. Therefore, the m.3243A>G mutation might considerably impede electron transfer upstream of CoQ, particularly through Complex I, despite the downregulation of multiple ETC proteins in Lu04 cybrids. By contrast, the m.8344A>G mutation markedly inhibited electron flow downstream of CoQ, as evident from the negligible OCR and COX II levels in the MERRF cybrids [22]. Although several nDNA-encoded ETC proteins were also suppressed in Lu04 cybrids, the severe reduction in the NDUFB8 level indicates that the most severe defects occur in Complex I. The reduced ubiquinol-10:ubiquinone-10 ratio may be also associated with reduced DHODH level in Lu04 cybrids. Guaras et al. reported that rotenone did not affect the ubiquinol:ubiquinone ratio but reversed the effect of AA [19]; however, they did not report the total CoQ level in the mouse cells. We previously analyzed ubiquinone-10 with the assumption that all ubiquinol-10 was oxidized during extended sample extraction and demonstrated that AA reduced CoQ_{10} levels in 143B cells [28]. However, the findings from the accurate CoQ analysis in the present study indicate that AA markedly increased the ubiquinol-10:ubiquinone-10 ratio and slightly increased the total CoQ_{10} levels. The pattern of changes in the total CoQ_{10} level in Lu04 cybrids and in the 143B cells treated with rotenone and AA was different from or independent of the pattern of changes in the ubiquinol-10:ubiquinone-10 ratio. Watanabe et al. [48] separately analyzed reduced and oxidized forms of CoQ_{10} in skin fibroblasts of patients with various mitochondrial diseases and concluded that the $CoQ_{10}H_2$/total CoQ_{10} ratio was higher in patients with Complexes IV and V deficiency than those with Complex I deficiency or the control group, but the ratio did not differ between the control group and the Complex I deficiency group [48]. Although that study did not use cybrids and combined patients with various gene defects other than primary CoQ_{10} deficiency into the same group, findings of this study consistently support the notion that Complex IV deficiency increases the ubiquinol:ubiquinone ratio.

In the current study, the reduced total CoQ_{10} levels in Lu04 cybrids might have resulted from the reduced levels of PDSS2, COQ3-a, COQ4, and COQ9, with the reductions being associated with the downregulation of their respective genes. The data might also have been influenced by mitochondrial energy deficiency. The observed upregulation of COQ8 in this study can be attributed to the upregulation of *COQ8* gene. However, the unchanged levels of COQ5, COQ6, and COQ7 in Lu04 cybrids indicate that changes in the levels of *PDSS* and *COQ* are not entirely dependent on the mRNA expression levels of their corresponding genes. The downregulation of PDSS and COQ genes, with the exception of *COQ2* and *COQ8*, may be partially, but not exclusively, attributable to the downregulation of *PPARGC1A* in Lu04 cybrids because we previously found that transient knockdown of *PPARGC1A* downregulated *PDSS2*, *COQ3*, *COQ4*, *COQ6*, *COQ8A*, and *COQ9* in 143B cells [37]. Xie et al. demonstrated that the expression of human COQ8A in the *coq8* mutants of *S. cerevisiae* partially restored the phosphorylation states of Coq3, Coq5, and Coq7 [49]. Furthermore, the overexpression of Coq8 was reported to restore the levels of Coq4, Coq7, and Coq9 in several yeast *coq* null mutants [50]. We previously found that FCCP treatment suppressed the COQ3-a level without affecting the COQ3-b level or *COQ3* expression in 143B cells and speculated that COQ3-a could be a phosphorylated isoform [23,24]. The upregulation of both *COQ8* gene and COQ8 protein expression in Lu04 cybrids could be a compensatory change in response to abnormal CoQ_{10} status and to the abnormal COQ3 phosphorylation status in Lu04 cybrids under the condition of mitochondrial energy deficiency.

A moderate (15 %) reduction was observed in the level of MNRR1 in Lu04 cybrids. This finding differs from that of Aras et al., who reported a nearly complete disappearance of MNRR1 in cybrids harboring 73 % of the m.3243A>G mutation [41]. Therefore, MNRR1-mediated signaling likely does not substantially contribute to the marked reduction in the level of *PPARGC1A* mRNA in Lu04 cybrids, although Aras et al. indicated that the level of PGC-1α can be regulated by MNRR1 [41]. Cotan et al. reported a reduction in cytochrome *c* levels in MELAS fibroblasts

with the m.3243A>G mutation, although they did not conduct experiments for cybrids [27]. Therefore, the substantial reductions in cytochrome *c* levels in Lu04 cybrids can be considered a novel finding. The signaling mediated by PGC-1α affects various downstream mitochondrial proteins through several common transcription factors [34,51]. The expression of genes encoding cytochrome *c*, TFAM, many nDNA-encoded subunits of OXPHOS complexes, VDAC1, and some subunits of translocases for mitochondrial import, including TOM20, can be regulated by PGC-1α through nuclear respiratory factor (NRF)-1 or NRF-2 [34,35,47,51–53]. Because the levels of TFAM, TOM20, and VDAC1 remained unchanged, we speculate that decreased cytochrome *c* levels in Lu04 cybrids are associated with dysregulation of other transcription factors other than NRF-1, such as those indicated by Scarpulia [51]. To the best of our knowledge, studies have yet to demonstrate the involvement of NRF-1 or NRF-2 in the regulation of *ATP5F1A*, the gene coding for ATP5A. One study observed increased protein levels of ATP5A and several subunits of OXPHOS complexes in long-lived endocrine mutant mice but these changes were associated with regulators other than PGC-1α [54]. The results of increased ATP5A levels, no alteration in mitochondrial mass, and unchanged protein levels of TOM20, VDAC1 and TFAM also suggest that there should be no extensive suppression of mitochondrial biogenesis in the Lu04 cybrids. PGC-1α-mediated signaling may contribute to the observed effects, but it is unlikely to be the primary factor influencing the reduction in all nDNA-encoded subunits of the four respiratory enzyme complexes in Lu04 cybrids.

Impaired protein import due to mitochondrial energy deficiency may reduce the levels of all nDNA-encoded proteins of the four respiratory enzyme complexes. It may be also the cause for the reduction in DHODH level observed in the current study, because the import of DHODH requires energy from mitochondrial membrane potential [18] and no association has been noted between DHODH regulation and PGC-1α. Furthermore, mtDNA-encoded OXPHOS subunits are crucial for the assembly of Complex I [55,56] and Complex IV [1]. Loguercio Polosa et al. showed that the cybrids harboring a high percentage of the m.3243A>G mutation had markedly reduced steady-state levels of COX I and NDUFB8 without a noticeable reduction in the level of ATP5A, SDHB, and UQCRC2 [11], although that study did not perform quantification analysis with multiple replicates for that Western blot analysis. The marked reduction in NDUFB8 level found in that study is consistent with our findings. Shoop et al. reported that eliminating the m.3243A>G mutation by using a mitochondria-targeted ARCUS nuclease in a cybrid line restored the protein levels of NDUFB8 [57]. These findings indicate that reductions in NDUFB8 protein levels constitute a sensitive indicator of the secondary defects in the nDNA-encoded subunits of Complex I resulted from the m.3243A>G mutation. Moreover, we observed a significant reduction (47 %) in the levels of NDUFS2 in Lu04 cybrids, a novel finding that confirms the abnormality of Complex I. Geffroy et al. reported that cybrids harboring the m.3243A>G mutation induced the accumulation of Complex I assembly intermediates containing NDUFS2 and caused a substantial reduction in the abundance of Complex I [10].

On the basis of our finding that TFAM levels remained unchanged in Lu04 cybrids, we speculate that the observed reduction in the steady-state levels of COX II and possibly other mtDNA-encoded proteins may be attributable to not only impaired mitochondrial protein synthesis but also severe mitochondrial energy deficiency-mediated secondary effects because we previously found that FCCP treatment reduced the level of both total CoQ_{10} levels and COX II in 143B cells [22]. Using an in vitro mitochondrial translation system, Clarson et al. also demonstrated that the chemical uncoupler carbonyl cyanide *m*-chlorophenylhydrazone, either alone or in combination with oligomycin, inhibited the formation of COX II and led to the accumulation of unprocessed COX II in the translation products [58]. Furthermore, mitochondrial energy deficiency may reduce the levels of mtDNA-encoded proteins by disrupting the import and maturation of certain nDNA-encoded respiratory enzyme subunits that are crucial for maintaining the levels of mtDNA-encoded proteins in the mitochondria. Cunatova et al. demonstrated that COX4I1 knockout markedly suppressed the steady-state levels of several nDNA-encoded subunits and mtDNA-encoded subunits of Complex IV in cells. The knockout not only reduced the contents of Complex IV and supercomplexes assembled from Complexes I, III, and IV but also suppressed the synthesis of most mtDNA-encoded proteins, with the exception of the two subunits of complex V [59]. In this study, we discovered that Lu04 cybrids exhibited markedly reduced levels of COX4I1, a novel finding that underscores the potential aggravating effect caused by COX4I1 reduction in cybrids harboring the m.3243A>G mutation.

In conclusion, this study reveals that secondary CoQ_{10} deficiency and reduced PDSS2 and various COQ proteins levels due to the m.3243A>G mutation are associated with defects in the mitochondrial respiratory chain and energy production of mitochondria in Lu04 cybrids. These changes are associated with reductions in cytochrome *c* and nDNA-encoded subunits of the respiratory enzyme complexes I, II, III, and IV, which may result from inhibited protein import due to mitochondrial energy deficiency although downregulation of *PPARGC1A* and other unknown dysregulated biogenesis pathways may be partially involved. The novel discovery of a reduced ubiquinol-10:ubiquinone-10 ratio in Lu04 cybrids and in rotenone-treated 143B cells suggests that the m.3243A>G mutation induces more pronounced defects in Complex I than in other respiratory complexes, leading to increased blockage in electron flow upstream of CoQ. We thus propose that a low ratio of ubiquinol-10 to ubiquinone-10 is a novel feature of MELAS syndrome caused by the m.3243A>G mutation. The observed reduction in the level of DHODH in Lu04 cybrids is also a novel finding that may also be a secondary effect arising from mitochondrial energy deficiency, potentially contributing to a reduction in the ubiquinol-10:ubiquinone-10 ratio and exacerbating the impairment of pyrimidine biosynthesis.

CRediT authorship contribution statement

Hsiu-Chuan Yen: Writing – review & editing, Writing – original draft, Visualization, Validation, Supervision, Resources, Project administration, Methodology, Investigation, Funding acquisition, Formal analysis, Conceptualization. **Chia-Tzu Hsu:** Validation, Methodology, Investigation, Formal analysis, Data curation. **Shin-Yu Wu:** Visualization, Validation, Investigation, Formal analysis, Data curation. **Chia-Chi Kan:** Investigation, Formal analysis, Data curation. **Hsing-Ming Chang:** Investigation, Formal analysis, Data curation. **Yu-An Chien:** Investigation, Data curation. **Yau-Huei Wei:** Writing – review & editing, Resources. **Chun-Yen Wu:** Investigation, Formal analysis, Data curation.

Declaration of competing interest

The authors declare that they have no known competing financial interests or personal relationships that could have appeared to influence the work reported in this paper.

Data availability

The data that has been used is confidential.

Acknowledgements

This research was funded by National Science and Technology Council, Taiwan (MOST 109-2320-B-182-035-MY3 and NSTC112-2320-B-182-051) and Chang Gung Memorial Hospital at Linkou, Taiwan (CMRPD1C0731, CMRPD1C0732, CMRPD1M0631, CMRPD1M0632, and BMRP532) to HCY. It was also supported by the Undergraduate Research Projects from National Science and Technology Council to CTH (107-2813-C-182-080-B), HMC (106-2813-C-182-034-B), and YAC (110-2813-C-182-031-B).

Appendix A. Supplementary data

Supplementary data to this article can be found online at https://doi.org/10.1016/j.bbabio.2024.149492.

References

[1] M. Brischigliaro, M. Zeviani, Cytochrome *c* oxidase deficiency, Biochim. Biophys. Acta Bioenerg. 1862 (2021) 148335.
[2] S. DiMauro, E.A. Schon, Mitochondrial disorders in the nervous system, Annu. Rev. Neurosci. 31 (2008) 91–123.
[3] S.M. Khan, R.M. Smigrodzki, R.H. Swerdlow, Cell and animal models of mtDNA biology: progress and prospects, Am. J. Phys. Cell Phys. 292 (2007) C658–C669.
[4] D.C. Wallace, Diseases of the mitochondrial DNA, Annu. Rev. Biochem. 61 (1992) 1175–1212.
[5] O. Russell, D. Turnbull, Mitochondrial DNA disease-molecular insights and potential routes to a cure, Exp. Cell Res. 325 (2014) 38–43.
[6] T. Suzuki, A. Nagao, T. Suzuki, Human mitochondrial diseases caused by lack of taurine modification in mitochondrial tRNAs, Wiley Interdiscip. Rev. RNA 2 (2011) 376–386.
[7] S.W. Schaffer, C.J. Jong, T. Ito, J. Azuma, Role of taurine in the pathologies of MELAS and MERRF, Amino Acids 46 (2014) 47–56.
[8] M. Picard, J. Zhang, S. Hancock, O. Derbeneva, R. Golhar, P. Golik, S. O'Hearn, S. Levy, P. Potluri, M. Lvova, A. Davila, C.S. Lin, J.C. Perin, E.F. Rappaport, H. Hakonarson, I.A. Trounce, V. Procaccio, D.C. Wallace, Progressive increase in mtDNA 3243A>G heteroplasmy causes abrupt transcriptional reprogramming, Proc. Natl. Acad. Sci. U. S. A. 111 (2014) E4033–E4042.
[9] C.Y. Pang, H.C. Lee, Y.H. Wei, Enhanced oxidative damage in human cells harboring A3243G mutation of mitochondrial DNA: implication of oxidative stress in the pathogenesis of mitochondrial diabetes, Diabetes Res. Clin. Pract. 54 (Suppl. 2) (2001) S45–S56.
[10] G. Geffroy, R. Benyahia, S. Frey, V. Desquiret-Dumas, N. Gueguen, C. Bris, S. Belal, A. Inisan, A. Renaud, A. Chevrollier, D. Henrion, D. Bonneau, F. Letournel, G. Lenaers, P. Reynier, V. Procaccio, The accumulation of assembly intermediates of the mitochondrial complex I matrix arm is reduced by limiting glucose uptake in a neuronal-like model of MELAS syndrome, Biochim. Biophys. Acta Mol. basis Dis. 2018 (1864) 1596–1608.
[11] P. Loguercio Polosa, F. Capriglia, F. Bruni, Molecular investigation of mitochondrial RNA19 role in the pathogenesis of MELAS disease, Life (Basel) 13 (2023) 1863.
[12] R.P. McMillan, S. Stewart, J.A. Budnick, C.C. Caswell, M.W. Hulver, K. Mukherjee, S. Srivastava, Quantitative variation in m.3243A > G mutation produce discrete changes in energy metabolism, Sci. Rep. 9 (2019) 5752.
[13] J. Garrido-Maraver, M.D. Cordero, I.D. Monino, S. Pereira-Arenas, A.V. Lechuga-Vieco, D. Cotan, M. De la Mata, M. Oropesa-Avila, M. De Miguel, J. Bautista Lorite, E. Rivas Infante, M. Alvarez-Dolado, P. Navas, S. Jackson, S. Francisci, J. A. Sanchez-Alcazar, Screening of effective pharmacological treatments for MELAS syndrome using yeasts, fibroblasts and cybrid models of the disease, Br. J. Pharmacol. 167 (2012) 1311–1328.
[14] A.M. Awad, M.C. Bradley, L. Fernandez-Del-Rio, A. Nag, H.S. Tsui, C.F. Clarke, Coenzyme Q_{10} deficiencies: pathways in yeast and humans, Essays Biochem. 62 (2018) 361–376.
[15] M. Kawamukai, Biosynthesis of coenzyme Q in eukaryotes, Biosci. Biotechnol. Biochem. 80 (2016) 23–33.
[16] M. Turunen, J. Olsson, G. Dallner, Metabolism and function of coenzyme Q, Biochim. Biophys. Acta 1660 (2004) 171–199.
[17] M. Alcazar-Fabra, P. Navas, G. Brea-Calvo, Coenzyme Q biosynthesis and its role in the respiratory chain structure, Biochim. Biophys. Acta 2016 (1857) 1073–1078.
[18] J. Rawls, W. Knecht, K. Diekert, R. Lill, M. Loffler, Requirements for the mitochondrial import and localization of dihydroorotate dehydrogenase, Eur. J. Biochem. 267 (2000) 2079–2087.
[19] A. Guaras, E. Perales-Clemente, E. Calvo, R. Acin-Perez, M. Loureiro-Lopez, C. Pujol, I. Martinez-Carrascoso, E. Nunez, F. Garcia-Marques, M.A. Rodriguez-Hernandez, A. Cortes, F. Diaz, A. Perez-Martos, C.T. Moraes, P. Fernandez-Silva, A. Trifunovic, P. Navas, J. Vazquez, J.A. Enriquez, The $CoQH_2$/CoQ ratio serves as a sensor of respiratory chain efficiency, Cell Rep. 15 (2016) 197–209.
[20] J.A. Stefely, D.J. Pagliarini, Biochemistry of mitochondrial coenzyme Q biosynthesis, Trends Biochem. Sci. 42 (2017) 824–843.
[21] E. Fernandez-Vizarra, M. Zeviani, Mitochondrial disorders of the OXPHOS system, FEBS Lett. 595 (2021) 1062–1106.
[22] H.C. Yen, Y.C. Liu, C.C. Kan, H.J. Wei, S.H. Lee, Y.H. Wei, Y.H. Feng, C.W. Chen, C. C. Huang, Disruption of the human COQ5-containing protein complex is associated with diminished coenzyme Q_{10} levels under two different conditions of mitochondrial energy deficiency, Biochim. Biophys. Acta 2016 (1860) 1864–1876.
[23] H.C. Yen, W.Y. Yeh, S.H. Lee, Y.H. Feng, S.L. Yang, Characterization of human mitochondrial PDSS and COQ proteins and their roles in maintaining coenzyme Q_{10} levels and each other's stability, Biochim. Biophys. Acta Bioenerg. 1861 (2020) 148192.
[24] S.W. Chen, C.C. Liu, H.C. Yen, Detection of suppressed maturation of the human COQ5 protein in the mitochondria following mitochondrial uncoupling by an antibody recognizing both precursor and mature forms of COQ5, Mitochondrion 13 (2013) 143–152.
[25] S. Sacconi, E. Trevisson, L. Salviati, S. Ayme, O. Rigal, A.G. Redondo, M. Mancuso, G. Siciliano, P. Tonin, C. Angelini, K. Aure, A. Lombes, C. Desnuelle, Coenzyme Q_{10} is frequently reduced in muscle of patients with mitochondrial myopathy, Neuromuscul. Disord. 20 (2010) 44–48.
[26] R. Montero, M. Grazina, E. Lopez-Gallardo, J. Montoya, P. Briones, A. Navarro-Sastre, J.M. Land, I.P. Hargreaves, R. Artuch, Coenzyme Q_{10} deficiency study group. Coenzyme Q_{10} deficiency in mitochondrial DNA depletion syndromes, Mitochondrion 13 (2013) 337–341.
[27] D. Cotan, M.D. Cordero, J. Garrido-Maraver, M. Oropesa-Avila, A. Rodriguez-Hernandez, L. Gomez Izquierdo, M. De la Mata, M. De Miguel, J.B. Lorite, E. R. Infante, S. Jackson, P. Navas, J.A. Sanchez-Alcazar, Secondary coenzyme Q_{10} deficiency triggers mitochondria degradation by mitophagy in MELAS fibroblasts, FASEB J. 25 (2011) 2669–2687.
[28] H.C. Yen, F.Y. Chen, S.W. Chen, Y.H. Huang, Y.R. Chen, C.W. Chen, Effect of mitochondrial dysfunction and oxidative stress on endogenous levels of coenzyme Q_{10} in human cells, J. Biochem. Mol. Toxicol. 25 (2011) 280–289.
[29] N. Pfanner, B. Warscheid, N. Wiedemann, Mitochondrial proteins: from biogenesis to functional networks, Nat. Rev. Mol. Cell Biol. 20 (2019) 267–284.
[30] V. Felipo, S. Grisolia, Precursors of mitochondrial proteins are degraded in the cytosol at different rates, FEBS Lett. 209 (1986) 227–230.
[31] H.C. Yen, B.S. Chen, S.L. Yang, S.Y. Wu, C.W. Chang, K.C. Wei, J.C. Hsu, Y.H. Hsu, T.H. Yen, C.L. Lin, Levels of coenzyme Q_{10} and several COQ proteins in human astrocytoma tissues are inversely correlated with malignancy, Biomolecules 12 (2022) 336.
[32] I. Kuhl, M. Miranda, I. Atanassov, I. Kuznetsova, Y. Hinze, A. Mourier, A. Filipovska, N.G. Larsson, Transcriptomic and proteomic landscape of mitochondrial dysfunction reveals secondary coenzyme Q deficiency in mammals, Elife 6 (2017) e30952.
[33] J.A. Villena, New insights into PGC-1 coactivators: redefining their role in the regulation of mitochondrial function and beyond, FEBS J. 282 (2015) 647–672.
[34] O. Abu Shelbayeh, T. Arroum, S. Morris, K.B. Busch, PGC-1α is a master regulator of mitochondrial lifecycle and ROS stress response, Antioxidants (Basel) 12 (2023) 1075.
[35] E. Mormeneo, C. Jimenez-Mallebrera, X. Palomer, V. De Nigris, M. Vazquez-Carrera, A. Orozco, A. Nascimento, J. Colomer, C. Lerin, A.M. Gomez-Foix, PGC-1α induces mitochondrial and myokine transcriptional programs and lipid droplet and glycogen accumulation in cultured human skeletal muscle cells, PLoS One 7 (2012) e29985.
[36] Z. Wu, P. Puigserver, U. Andersson, C. Zhang, G. Adelmant, V. Mootha, A. Troy, S. Cinti, B. Lowell, R.C. Scarpulla, B.M. Spiegelman, Mechanisms controlling mitochondrial biogenesis and respiration through the thermogenic coactivator PGC-1, Cell 98 (1999) 115–124.
[37] H.C. Yen, C.C. Liu, C.C. Kan, C.S. Chen, H.R. Wei, Suppression of coenzyme Q_{10} levels and the induction of multiple PDSS and COQ genes in human cells following oligomycin treatment, Free Radic. Res. 48 (2014) 1125–1134.
[38] J. Garrido-Maraver, M.V. Paz, M.D. Cordero, J. Bautista-Lorite, M. Oropesa-Avila, M. de la Mata, A.D. Pavon, I. de Lavera, E. Alcocer-Gomez, F. Galan, P. Ybot Gonzalez, D. Cotan, S. Jackson, J.A. Sanchez-Alcazar, Critical role of AMP-activated protein kinase in the balance between mitophagy and mitochondrial biogenesis in MELAS disease, Biochim. Biophys. Acta 1852 (2015) 2535–2553.
[39] S. Aras, H. Arrabi, N. Purandare, M. Huttemann, J. Kamholz, S. Zuchner, L. I. Grossman, Abl2 kinase phosphorylates bi-organellar regulator MNRR1 in mitochondria, stimulating respiration, Biochim. Biophys. Acta, Mol. Cell Res. 2017 (1864) 440–448.
[40] S. Aras, M. Bai, I. Lee, R. Springett, M. Huttemann, L.I. Grossman, MNRR1 (formerly CHCHD2) is a bi-organellar regulator of mitochondrial metabolism, Mitochondrion 20 (2015) 43–51.
[41] S. Aras, N. Purandare, S. Gladyck, M. Somayajulu-Nitu, K. Zhang, D.C. Wallace, L. I. Grossman, Mitochondrial Nuclear Retrograde Regulator 1 (MNRR1) rescues the cellular phenotype of MELAS by inducing homeostatic mechanisms, Proc. Natl. Acad. Sci. U. S. A. 117 (2020) 32056–32065.
[42] C.Y. Liu, C.F. Lee, C.H. Hong, Y.H. Wei, Mitochondrial DNA mutation and depletion increase the susceptibility of human cells to apoptosis, Ann. N. Y. Acad. Sci. 1011 (2004) 133–145.
[43] M.P. King, G. Attardi, Isolation of human cell lines lacking mitochondrial DNA, Methods Enzymol. 264 (1996) 304–313.
[44] B.H. Robinson, Use of fibroblast and lymphoblast cultures for detection of respiratory chain defects, Methods Enzymol. 264 (1996) 454–464.
[45] T.H. Yen, C.W. Chang, H.R. Tsai, J.F. Fu, H.C. Yen, Immunosuppressive therapies attenuate paraquat-induced renal dysfunction by suppressing inflammatory responses and lipid peroxidation, Free Radic. Biol. Med. 191 (2022) 249–260.
[46] H.C. Yen, Y.T. Hsu, Impurities from polypropylene microcentrifuge tubes as a potential source of interference in simultaneous analysis of multiple lipid-soluble antioxidants by HPLC with electrochemical detection, Clin. Chem. Lab. Med. 42 (2004) 390–395.
[47] S.S. Dhar, S. Ongwijitwat, M.T.T. Wong-Riley, Nuclear respiratory factor 1 regulates all ten nuclear-encoded subunits of cytochrome *c* oxidase in neurons, J. Biol. Chem. 283 (2008) 3120–3129.
[48] C. Watanabe, H. Osaka, M. Watanabe, A. Miyauchi, E.F. Jimbo, T. Tokuyama, H. Uosaki, Y. Kishita, Y. Okazaki, T. Onuki, T. Ebihara, K. Aizawa, K. Murayama, A. Ohtake, T. Yamagata, Total and reduced/oxidized forms of coenzyme Q_{10} in fibroblasts of patients with mitochondrial disease, Mol. Genet. Metab. Rep. 34 (2023) 100951.
[49] L.X. Xie, E.J. Hsieh, S. Watanabe, C.M. Allan, J.Y. Chen, U.C. Tran, C.F. Clarke, Expression of the human atypical kinase ADCK3 rescues coenzyme Q biosynthesis and phosphorylation of Coq polypeptides in yeast coq8 mutants, Biochim. Biophys. Acta 2011 (1811) 348–360.

[50] L.X. Xie, M. Ozeir, J.Y. Tang, J.Y. Chen, S.K. Jaquinod, M. Fontecave, C.F. Clarke, F. Pierrel, Overexpression of the Coq8 kinase in *Saccharomyces cerevisiae coq* null mutants allows for accumulation of diagnostic intermediates of the coenzyme Q_6 biosynthetic pathway, J. Biol. Chem. 287 (2012) 23571–23581.
[51] R.C. Scarpulla, Transcriptional paradigms in mammalian mitochondrial biogenesis and function, Physiol. Rev. 88 (2008) 611–638.
[52] D.C. Wright, D.H. Han, P.M. Garcia-Roves, P.C. Geiger, T.E. Jones, J.O. Holloszy, Exercise-induced mitochondrial biogenesis begins before the increase in muscle PGC-1α expression, J. Biol. Chem. 282 (2007) 194–199.
[53] F. Guarino, F. Zinghirino, L. Mela, X.G. Pappalardo, F. Ichas, V. De Pinto, A. Messina, NRF-1 and HIF-1α contribute to modulation of human VDAC1 gene promoter during starvation and hypoxia in HeLa cells, Biochim. Biophys. Acta Bioenerg. 1861 (2020) 148289.
[54] A.M. Elmansi, R.A. Miller, Coordinated transcriptional upregulation of oxidative metabolism proteins in long-lived endocrine mutant mice, Geroscience 45 (2023) 2967–2981.
[55] C. Ugalde, R.H. Triepels, M.J. Coenen, L.P. van den Heuvel, R. Smeets, J. Uusimaa, P. Briones, J. Campistol, K. Majamaa, J.A. Smeitink, L.G. Nijtmans, Impaired complex I assembly in a Leigh syndrome patient with a novel missense mutation in the ND6 gene, Ann. Neurol. 54 (2003) 665–669.
[56] L. Sanchez-Caballero, S. Guerrero-Castillo, L. Nijtmans, Unraveling the complexity of mitochondrial complex I assembly: a dynamic process, Biochim. Biophys. Acta 2016 (1857) 980–990.
[57] W.K. Shoop, J. Lape, M. Trum, A. Powell, E. Sevigny, A. Mischler, S.R. Bacman, F. Fontanesi, J. Smith, D. Jantz, C.L. Gorsuch, C.T. Moraes, Efficient elimination of MELAS-associated m.3243G mutant mitochondrial DNA by an engineered mitoARCUS nuclease, Nat. Metab. 5 (2023) 2169–2183.
[58] G.H. Clarkson, R.O. Poyton, A role for membrane potential in the biogenesis of cytochrome c oxidase subunit II, a mitochondrial gene product, J. Biol. Chem. 264 (1989) 10114–10118.
[59] K. Cunatova, D.P. Reguera, M. Vrbacky, E. Fernandez-Vizarra, S. Ding, I. M. Fearnley, M. Zeviani, J. Houstek, T. Mracek, P. Pecina, Loss of COX4I1 leads to combined respiratory chain deficiency and impaired mitochondrial protein synthesis, Cells 10 (2021) 369.